EUROPEAN ORGANIZATION FOR NUCLEAR RESEARCH
CERN - SPS DIVISION

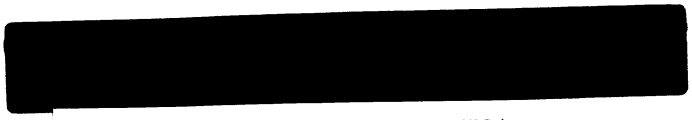

CERN SPS/AOP/78-9

The SPS Chromaticity and its correction with lumped sextupoles.

Y. Baconnier, M. Cornacchia, L. Evans, P.E. Faugeras, A. Faugier,
J. Gareyte and A. Hilaire

Abstract. SPS Chromaticities have been carefully measured on both 10 GeV/c and 200 GeV/c platforms, as well as during the magnetic field rise. The linear part of the tune variation with momentum ("linear" chromaticity) thus obtained has been used to refine the model which allows a very accurate compensation of both chromaticities in the low energy part of the cycle. An important non-linear variation of the tune with $\Delta p/p$ has been shown to take place in the horizontal plane. This effect now well known to the designers of large e-p storage rings, arises from the particular sextupole distribution used to compensate the linear chromaticities: because of the relatively small number of sextupoles, the distribution is rich in harmonics other than zero, and some of them are responsible for the non-linear effects. Both analytic calculations and computer simulation with the AGS program clearly show how this occurs, and what could be the eventual cures, should this curvature of chromaticity be detrimental to the functioning of the machine. A larger number of sextupoles would be needed for perfect compensation.

Geneva, 29th May, 1978

TABLE OF CONTENTS

INTRODUCTION

Up to now some part of the injected beam is always lost during the early part of the acceleration cycle of the SPS, i.e. from injection up to transition. These losses, which cannot be attributed to particles not trapped by the accelerating system, have been partially reduced by a careful adjustment of the machine parameters and are acceptable for the actual mode of operation - one CPS pulse injection - but they become much stronger when one tries to inject two CPS batches in the SPS. In this case important losses can clearly be seen during the longer injection platform [1].

Some possible explanations for these losses have been proposed, [2] and, as suggested in this report, a systematic experimental study of the beam behaviour in the transverse planes was undertaken in order to understand the mechanism of the losses. In the course of these experiments it was found that the machine sextupoles, used for chromaticity adjustment, induce a non linear variation of the betatron tunes Q_H, Q_V with the momentum deviation $\Delta p/p$ of the beam, mainly in the horizontal plane.

Although this effect alone cannot explain all the observed beam losses, it is sufficiently important in itself to be studied carefully, which is the subject of this report. We will review first the experimental observations which show the prime influence of the chromaticity sextupoles on the curvature of the betatron tunes. In chapter 2, we will use the computer program AGS, [3] to simulate this effect, which permits to separate the various contributions to the curvature of the chromaticity curves. Recent developments on accelerator theory have given analytical expression for the non linear part of the chromaticity. This is summarized in chapter 3, where these theoretical expressions are compared and found to be in agreement with the results of AGS calculations. In the next chapter, simulation of the SPS with the AGS program is used to analyse the experimental data. Extrapolation of these results allows to show how far one can correct this non linear chromaticity, which has to be taken into account for the SPS intensity improvement program, as well as for future developments like the p-$\bar{p}$ project.

1. REVIEW OF EXPERIMENTAL RESULTS

1.1 Observation of a non linear chromaticity in the SPS

This study was started by looking first at the losses which occurred at a merely constant rate during the 1.2 sec long injection flat bottom used for double batch injection experiments. In the normal single injection mode, losses are also present during that part of the cycle, but are less detrimental as the flat bottom is much shorter.

The first step was to verify that the chromaticity of the machine is properly compensated by the LSF and LSD sextupoles set to their nominal values, [5]. One then measured the dependence of Q_H and Q_V

with the beam momentum, which was varied by changing the mean radial position of the beam with the radial loop of the RF control system. This immediately revealed a strong dissymmetry of the machine in the radial plane, as shown by the dashed curves on Fig. 1: while Q_V remains practically constant over the whole range of beam displacements, Q_H increases for negative radial displacements reaching the $3Q_H = 80$ resonance for a mean radial position of about $\Delta\bar{R} = -10$ mm, where the full beam is lost. Similarly the 50 % transmission points are obtained for $\Delta\bar{R} = -7.5$ mm and $\Delta\bar{R} = +19$ mm. Moreover, the available radial displacement for $\Delta\bar{R} < 0$ is further reduced if one tries to go back to the nominal working point $Q_H = 26.62$, $Q_V = 26.58$.

The possibility of a physical obstruction in the vacuum chamber was completely eliminated after a survey of the vacuum chamber aperture around the ring made by the operations staff with a local closed orbit bump at each quadrupole location, which gave no result.

If such a non linear variation of Q_H with momentum is due to some localized magnetic defect, one should observe a strong reduction in the transverse machine acceptance. This was checked by the kicking beam technique, [4], in which one blows up a pencil beam in a controlled fashion with the Q-measuring kickers and looks at the resulting transmission one second after the kick. As compared to the results of Commissioning Report No. 50, the horizontal kick amplitude for 50 % transmission is reduced by a factor of two, whereas such a reduction cannot be seen in the vertical plane (see Fig. 2, curves 1 and 2).

Soon after, however, the Main Ring Group discovered that because of a burnt connection, half of the LSF sextupoles around the ring were not powered, while the other half was fed with twice the nominal current. When this fault was repaired, the working space in the Q_H, Q_V diagram became larger and the horizontal dynamic aperture greatly improved as shown by curve No. 4 on Fig. 2, which compares favourably with previous measurements.

To the contrary, the non linear variation of Q_H with the mean radial position remained exactly the same (continuous curves of Fig. 1) and had still to be explained: when measuring the dynamic transverse aperture, it was found that the betatron tunes Q_H and Q_V are independent of the amplitude of the applied kick up to at least the 50 % transmission points, i.e. 40 mm horizontal and 15 mm vertical. This shows that there is no stray octupolar field in the machine which could be responsible for this curvature: the Landau damping octupoles powered at the level necessary to damp the resistive wall instability, ($\simeq 4A$, which produces a Q-spread of about $2.5\ 10^{-3}$) give $\Delta Q_H = 2.5 \times 10^{-4} (\Delta R)^2$, ΔR in cm, i.e. an effect much smaller than the one measured.

It should finally be noted that the losses during the injection flat bottom were strongly reduced with the correct connection of the LSF sextupoles, but not the loss during the front porch.

1.2 Calibration of the radial steering

Before studying in detail this non linear chromaticity effect, one has to examine how the chromaticity is measured. Usually one displaces the orbit of the beam off centre by an RF bump on the radial loop of the RF control system. The resulting change Δp in the beam momentum with respect to the equilibrium value p is related to the change ΔR of the mean radial position of the beam by, [6] :

$$\frac{\Delta p}{p} = \gamma_{tr}^2 \cdot \frac{\Delta R}{R} \qquad (1)$$

assuming that there is no field variation. With R = 1100 m and for the present working point $Q_H = 26.62$, $Q_V = 26.57$, the kinetic energy at transition is $\gamma_{tr} = 23.23$ which gives :

$$\frac{\Delta p}{p}_{(‰)} = .4906 . \Delta R_{(mm)} \qquad (2)$$

Such an orbit displacement may induce changes $\Delta Q_H, \Delta Q_V$ in the betatron wave number Q_H, Q_V from which the chromaticity ξ_H, ξ_V are calculated by :

$$\frac{\Delta Q_H}{Q_H} = \xi_H \cdot \frac{\Delta p}{p} \qquad \frac{\Delta Q_V}{Q_V} = \xi_V \cdot \frac{\Delta p}{p} \qquad (3)$$

The mean radial position of the beam is measured by the beam position pick-ups BP's, distributed around the ring, [7]. The effect of residual closed orbit distortion is eliminated by acquiring the displaced orbit and substracting from it the central orbit acquired just after or just before the RF radial bump as shown on Fig. 3.

Nevertheless this method has several limitations :

- the BP's gain must be properly adjusted and calibrated for each beam intensity, in order to avoid saturation in the measuring chain, especially for the sum signal. Also all the BP's must be working at the same time.

- for large beam excursions, the BP's are no longer linear. This is particularly important at locations where the momentum compaction function α_p is maximum (see Fig. 3b).

- fluctuations from pulse to pulse require several measurements to get a good accuracy.

One has then calibrated the amplitude $\Delta\bar{R}$ of the required RF radial bump against the mean radial position ΔR measured by the BP's for different energies and for $-20 \text{ mm} \leqslant \Delta\bar{R} \leqslant 20 \text{ mm}$ (ten measurements per value of $\Delta\bar{R}$). This gives :

$$\Delta R_{BP} = (1.142 \pm .050).\Delta\bar{R} \qquad (4)$$

A cross-calibration of the radial steering was also made by measuring the actual accelerating frequency f versus $\Delta\bar{R}$, which is related to the mean radial position by, [6] :

$$\frac{\Delta B}{B} = \gamma^2 \frac{\Delta f}{f} + (\gamma^2 - \gamma_{tr}^2) \frac{\Delta R}{R} \qquad (5)$$

which for $\Delta B = 0$ reduces to :

$$\frac{\Delta R}{R} = - \frac{\gamma^2}{\gamma^2 - \gamma_{tr}^2} \cdot \frac{\Delta f}{f} \qquad (5')$$

For the same range of RF bump amplitudes $\Delta\bar{R}$ as above, one has obtained :

$$\Delta R_{RF} = (1.095 \pm .015).\Delta\bar{R} \qquad (6)$$

The small discrepancy between (4) and (6) is within the experimental errors, but as frequency measurements are more accurate, (6) will be used throughout this report as calibration factor of the radial steering. In practice we will have :

$$\frac{\Delta p}{p}_{(‰)} = .537.\Delta\bar{R}_{(mm)} \qquad (2')$$

and

$$\xi_{H,V} = \frac{\Delta Q_{H,V}}{Q_{H,V}} \cdot \frac{1.862}{\Delta\bar{R}_{(mm)}} \qquad (4')$$

1.3 Source of the non linear chromaticity

One has to find now which parameters of the machine influence this non linear variation of the betatron tunes with the beam momentum deviation. All the experiments reported below were done at a relatively low intensity of 2.10**12 p injected, with all the extraction elements switched off, as well as the harmonic correctors and the Landau damping octupoles. Only the active dampers were kept on. In this way one eliminates any possible stray effect coming from high order lenses, and the chromaticities should be practically independent of $\Delta p/p$, their value being determined by the amount of correction applied by the chromaticity sextupoles LSF and LSD.

With these LSF, LSD sextupoles powered at their nominal operation settings, one found first that at 10 GeV, changing the nominal working point within the available space in the Q_H, Q_V diagram does not change the curvature of the curve Q_H versus $\Delta\bar{R}$. As it can be seen on Fig. 4a, the only noticeable change is that the maximum permitted beam displacement is increased when the central value of Q_H for $\Delta\bar{R} = 0$ is lowered to 26.59, as one is further away from the $3Q_H = 80$ stop band.

Measuring the chromaticity on the 200 GeV flat top under the same conditions shows that this non linear effect is also present, but that the curvature is less pronounced (Fig. 4b). For the nominal sextupoles settings, the horizontal chromaticity is practically zero for $\Delta\bar{R} \gg 0$, whereas it is about -.3 for $\Delta\bar{R} \ll -2.5$ mm. One can correct this residual chromaticity by adding a correction of $\Delta\xi_H = +.3$ to the sextupoles settings, but then one gets a positive chromaticity of about $\xi_H = +.3$ for $\Delta\bar{R} \gg 0$ (dashed curve of Fig. 4b). This effect does not exist in the vertical plane, but was also observed in the horizontal plane at 10 GeV.

The next step is to look at the bare machine, i.e. with the chromaticity sextupoles switched off. This is more easily done at 200 GeV where the smaller momentum spread and beam emittances allow larger excursion in tunes. As shown by the continuous curves of Fig. 5, Q_H and Q_V vary perfectly linearly with the mean radial position, from which the natural chromaticities of the machine at 200 GeV can be deduced :

$$\xi_H = -1.097 \qquad \xi_V = -1.358 \qquad (7)$$

which is fairly close to previous measurements, [5].

In order to definitely prove that the non linear chromaticity comes from the chromaticity sextupoles only, one then adjusted the LSF and LSD such as to make a correction of $\Delta\xi_H = +.50$ and $\Delta\xi_V = +1.46$. One sees on the dashed curves of Fig. 5 that while the vertical chromaticity is constant although slighlty overcompensated, there is a kink at $\Delta\bar{R} = 0$ in the curve $Q_H(\Delta\bar{R})$, corresponding to a jump in the residual horizontal chromaticity of $\Delta\xi_H = +.1$.

As there is no evidence of a magnetic defect in the LSF and LSD sextupoles, which were carefully tested, [8], one can conclude that this observed non linear effect is intrinsically linked to the way the chromaticity is corrected in the SPS, its amplitude being roughly proportional to the amount of correction applied.

2. SPS SIMULATION WITH THE AGS PROGRAMME

The AGS computer program allows the calculation of the betatron and dispersion functions of any alternating gradient synchrotron, [3]. All the calculations reported in this chapter were performed using a lattice structure with a super periodicity of 6, i.e. by neglecting here the effect of the enlarged quadrupoles which are placed in the even long straight section of the SPS. For the quadrupole gradients adjusted such as to get :

$$Q_H = 26.600 \ , \quad Q_V = 26.550$$

AGS gives a natural chromaticity of :

$$\xi_H = -1.262 \ , \quad \xi_V = -1.260 \tag{8}$$

If we insert in the structure chromaticity sextupoles as in the real SPS, i.e. one LSF in front of the quadrupoles QF - 02, 08, 14, 20, 26 and 32 in each sextant and one LSD half a magnetic period downstream of each LSF, and if we adjust their normalized strengthes (in m^{-3}) :

$$S_{LSF,LSD} = -\frac{1}{B\rho} \cdot \left(\frac{\partial^2 B}{\partial x^2}\right)_{LSF,LSD} \tag{9}$$

($B\rho$ is the magnetic rigidity for $\Delta p/p = 0$) such as to compensate the chromaticities (8), we obtain the continuous curves of Fig.6, which are similar to what has been measured: Q_H versus $\Delta p/p$ exhibits a strong curvature but this effect is much less pronounced for Q_V. Also, by changing slightly the sextupole strengthes S_{LSF}, S_{LSD}, Q_H reaches its minimum for $\Delta p/p \neq 0$, as was measured in Fig. 4.

Detailed calculations have permitted to separate the different contributions to this curvature as explained below.

2.1 Effect of the sextupole distribution

As the sextupole distribution follows the SPS super periodicity of 6 their effect can be assimilated to a set of periodic perturbations whose spacial frequencies are all the harmonics of the super periodicity. One of these harmonics, namely the 54th coincides with the $2\,Q_H = 54$ stop band which is not far from the nominal working point $Q_H = 26.60$. This leads to an attraction of Q_H into the half integer stop band at 27 for off-momentum particles and to a change in the horizontal betatron amplitude β_H, especially its maximum $\hat{\beta}_H$, which is effectively shown by the computer simulation (Fig. 7).

Fortunately, the regular pattern in the sextupole distribution allows to split the LSF sextupoles into two interlaced families such as LSF1, LSF2, LSF1, LSF2, ..., which are in antiphase as far as the 54th harmonic of their respective distribution is concerned. One can therefore try to excite these two sextupole families with two different strengthes S_{LSF1} and S_{LSF2}, in such a way that :

- the natural machine chromaticity is properly compensated,
- the effect of the 54th harmonic is minimized.

The sextupole strengthes are determined by calculating the change in tune due to the sextupoles for an off-momentum particle, [9] :

$$\delta Q_H = \frac{1}{4\pi}\int_C \beta_H(s)\, x(s)\, S(s)\, ds \qquad (10)$$

where $x(s) = \alpha_p(s)\,\Delta p/p$ is the particle position and S(s) the sextupolar correction around the ring. In our case, (10) can be reduced to :

$$\delta Q_H = -\frac{1}{4\pi}\left[\sum_{LSF1,LSF2,LSD} \beta_H.\alpha_p.\ell.S\right].\frac{\Delta p}{p} \qquad (11)$$

ℓ being the length of a sextupole of strength S. Using the lattice functions calculated with AGS at each sextupole location, the first condition leads to :

$$6.443*S_{LSF1} + 4.333*S_{LSF2} = 10.776*S_{LSF} \qquad (12)$$

where S_{LSF} is the LSF strength required for chromaticity correction when there is only one family. ($S_{LSF} = -.150\ m^{-3}$ for curve A of Fig. 6.) The second condition implies :

$$6.443*S_{LSF1} - 4.333*S_{LSF2} = 0 \qquad (13)$$

from which one obtains :

$$S_{LSF1} = -.1254\ m^{-3},\ S_{LSF2} = -.1865\ m^{-3} \qquad (14)$$

These values are very close to those calculated with AGS, which minimize the variation of $\hat{\beta}_H$ with $\Delta p/p$ (Fig. 7). With these values and with $S_{LSD} = .292\ m^{-3}$ (as for curve A) one obtains the curve B of Fig. 6. Although the curvature of Q_H versus $\Delta p/p$ is reduced, it is not completely eliminated, which means that other harmonics are also important (see chapter 3) but cannot be eliminated this way. Splitting also the LSD's into two families does not help either, as it was verified with AGS: as the LSD's are located half a magnetic period downstream of each LSF, they are in quadrature with respect to the 54th harmonic of the LSF distribution. Moreover their local β_H value is close to β_H minimum, which means that their contribution is small anyway.

2.2 Variation of β_H and α_p with $\Delta p/p$

In a linear machine, the contribution of the chromaticity sextupoles to the change δQ_H in tune for an off-momentum particle is obtained by putting in (11) the lattice functions β_H and α_p which corresponds to the central orbit. To the contrary, the Q_H value given by AGS is calculated by integration of (10) along the particle trajectory, using the lattice functions determined for each momentum deviation.

As shown on the bottom graph of Fig. 7 for one particular sextupole location, the momentum dispersion function $\alpha_p(s)$ varies practically linearly with $\Delta p/p$. Similarly, but to a lesser extent, the betatron function β_H also varies with $\Delta p/p$, even in the case of two LSF families, adjusted to minimize this variation. In other words, the effect of the sextupoles is different from what was expected because of the variation of the lattice functions with the momentum deviations, due to the sextupoles themselves.

In order to see if this variation of the lattice functions with $\Delta p/p$ explains the residual curvature, one can calculate its magnitude with (11) and substract it from curve B. For instance, the LSF1 family gives a correction :

$$\delta Q_{H_{LSF1}} = -\frac{1}{4\pi} \cdot \ell_{LSF1} \cdot S_{LSF1} \cdot \frac{\Delta p}{p} \sum_{LSF1} \left[\beta_H \cdot \alpha_p \,(\text{sext. on}) - \beta_H \cdot \alpha_p \,(\text{sext. off}) \right] \qquad (15)$$

Substracting (15) from curve B of Fig. 6 gives the curve C. The same correction, calculated for the LSF2 and LSD families successively lead to curves D and E respectively.

2.3 Bare machine

The curve of Fig. 6 still exhibits a small curvature, which comes from the little variations of the lattice functions with $\Delta p/p$, which are observed for the bare machine, i.e. the machine without any sextupole correction. In this case, AGS shows a variation of ± 3 % for α_p and of $\pm .5$ % for β_H, when $\Delta p/p$ varies by ± 1.5 % (Fig. 7, bottom graph). When plotting Q_H versus $\Delta p/p$ in this case, one obtains a slight curvature in comparison with a perfectly linear machine, i.e. a machine with a constant chromaticity of $\xi_H = -1.262$. Here again the magnitude of this effect can be characterized by :

$$\begin{aligned} \delta Q_H &= Q_H \left(\frac{\Delta p}{p}\right)_{AGS} - Q_H(0) \left[1 + \xi_H \left(\frac{\Delta p}{p} = 0\right) \cdot \frac{\Delta p}{p} \right] \\ &= Q_H \left(\frac{\Delta p}{p}\right)_{AGS} - 26.600 \left[1 - 1.262 \cdot \frac{\Delta p}{p} \right] \end{aligned} \qquad (16)$$

One can also substract this correction (16) from curve E. This gives the final curve F, which is practically flat, the residual fluctuations being within the accuracy of the calculation of the different corrections.

So far, we have looked only at the horizontal chromaticity as this is the one with the strongest non linear behaviour, but the same exercise could be performed on the Q_v curve. It remains to be seen if AGS calculation can be fitted with the SPS experimental data, which will be done in chapter 4.

3. ANALYTIC CALCULATION OF THE CHROMATICITY

The non linear part of the chromaticity can be calculated by developing the Courant and Snyder equation to the second and if necessary to the third order in momentum deviation $\delta = \Delta p/p_o$ [10],[11]. We will briefly recall the derivation of the formulae and then apply them to the SPS.

3.1 Derivation of the formulae

In the presence of field perturbations δB, the equation of the horizontal betatron motion for a particle of momentum $p = p.(1+\delta)$, is, [17] :

$$\frac{d^2x}{ds^2} + \left[\frac{1}{\rho^2} + K(s)\right]x = \frac{1}{\rho}\cdot\frac{\Delta p}{p} - \frac{1}{\rho}\cdot\frac{\delta B}{B} \qquad (17)$$

By limiting δB to sextupolar fields and developing in δ, (17) can be written as :

$$\frac{d^2x}{ds^2} + \left(\frac{1}{\rho^2} + K\right)x = \frac{1}{\rho}\left(\delta - \delta^2 + \cdots\right) + Kx\left(\delta - \delta^2 + \ldots\right) - \frac{S}{2}x^2\left(1 - \delta + \delta^2 - \ldots\right) \qquad (17')$$

where - ρ is the bending radius, B is the magnetic field

- $K(s) = B'/B\rho$ is the focusing parameter
- $S(s) = B''/B\rho$ is the normalized sextupole strength

The transverse displacement $x(s)$ is equal to the sum of the betatron amplitude x_β and the closed orbit deviation $\alpha_p\delta$. With the usual Courant and Snyder transformation, [12] :

$$x = \tilde{x}\beta_o^{1/2} \qquad \alpha_p = \tilde{\alpha}_p\beta_o^{1/2} \qquad d\phi = \frac{ds}{\nu_o\beta_o} \qquad (18)$$

this equation becomes :

$$\frac{d^2\tilde{x}}{d\phi^2} + \nu_o^2 \tilde{x} = \frac{1}{\rho}(\delta-\delta^2)\nu_o^2 \beta_o^{3/2} + K(\delta-\delta^2)\nu_o^2 \beta_o^2 \tilde{x} - \frac{S}{2}(1-\delta+\delta^2)\nu_o^2 \beta_o^{5/2} \tilde{x}^2 \quad (19)$$

where β_o and ν_o are the betatron function and tune for the central particle (δ=0). Note that ν_o was called $Q_H(\Delta p/p=0)$ in the previous chapter. In writing :

$$x = x_\beta + \alpha_p \delta \iff \tilde{x} = \tilde{x}_\beta + \tilde{\alpha}_p \delta \quad (20)$$

and with

$$\alpha_p = \alpha_{p_o} + \alpha_{p_1}\delta + \cdots \iff \tilde{\alpha}_p = \tilde{\alpha}_{p_o} + \tilde{\alpha}_{p_1}\delta + \cdots \quad (21)$$

we can find from (19) separate equations for $\tilde{x}_\beta$ and $\tilde{\alpha}_{p_o}, \tilde{\alpha}_{p_1}$:

$$\frac{d^2\tilde{x}_\beta}{d\phi^2} + \nu_o^2 \tilde{x}_\beta = (K - S\alpha_p).(\delta-\delta^2)\nu_o^2 \beta_o^2 \tilde{x}_\beta + \varepsilon(\delta).\tilde{x}_\beta^2 \quad (22)$$

$$\frac{d^2\tilde{\alpha}_{p_o}}{d\phi^2} + \nu_o^2 \tilde{\alpha}_{p_o} = \frac{\nu_o^2}{\rho} \cdot \beta_o^{3/2} \quad (23)$$

$$\frac{d^2\tilde{\alpha}_{p_1}}{d\phi^2} + \nu_o^2 \tilde{\alpha}_{p_1} = \nu_o^2 \beta_o^{3/2}\left(-\frac{1}{\rho} + K\alpha_{p_o} - \frac{S}{2}\alpha_{p_o}^2\right) \quad (24)$$

(22) is the betatron equation. Let us write :

$$(S\alpha_p - K)(\delta-\delta^2) = a(\phi).\delta + b(\phi).\delta^2 \quad (25)$$

with :

$$a(\phi) = \nu_o^2 \beta_o^2 (S\alpha_{p_o} - K)$$
$$b(\phi) = \nu_o^2 \beta_o^2 (S\alpha_{p_1} - S\alpha_{p_o} + K) \quad (26)$$

$a(\phi)$ and $b(\phi)$ being periodic in ϕ can be expanded in Fourier series :

$$a(\phi) = \bar{a} + \sum_{n\neq 0} a_n e^{in\phi} \qquad b(\phi) = \bar{b} + \sum_{n\neq o} b_n e^{in\phi} \quad (27)$$

In reference 10, the betatron equation is then solved by a successive approximation technique, which results in the perturbated tune :

$$\nu^2 = \nu_o^2 + \bar{a}\,\delta + \left[2\sum_{n>0} \frac{a_n^2}{n^2 - 4\nu_o^2} + \bar{b}\right]\delta^2 \qquad (28)$$

The solution for $\tilde{\alpha}_{p_o}$ and $\tilde{\alpha}_{p_1}$ are easily found :

$$\tilde{\alpha}_{p_o} = \nu_o^2 \sum_n \frac{F_n^o}{\nu^2 - n^2} \cdot e^{in\phi} \qquad (29)$$

$$\tilde{\alpha}_{p_1} = -\tilde{\alpha}_{p_o} + \nu_o^2 \sum_n \frac{F_n^1}{\nu^2 - n^2} \cdot e^{in\phi} \qquad (30)$$

where F_n^o and F_n^1 are the Fourier components of the functions F^o and F^1 respectively :

$$F^o = \frac{\beta_o^{3/2}}{\rho} \qquad F^1 = \beta_o^{3/2}\left(\alpha_{p_o} k - \frac{S}{2}\alpha_{p_o}^2\right) \qquad (31)$$

(28) can be rewritten as :

$$\nu^2 - \nu_o^2 \simeq 2\nu_o \cdot \Delta\nu = \bar{a}\,\delta + \left[2\sum_{n>0} \frac{a_n^2}{n^2 - 4\nu_o^2} + \bar{b}\right]\delta^2 \qquad (28')$$

The first term on the right hand side of (28') gives the usual linear chromaticity :

$$\xi = \frac{\Delta\nu}{\nu} \cdot \frac{1}{\delta} \simeq \frac{\bar{a}}{2\nu^2} \qquad (32)$$

with

$$\bar{a} = \frac{1}{2\pi}\int_o^{2\pi} \nu_o^2 \beta_o^2 (S\alpha_{p_o} - k)\, d\phi = \frac{\nu_o}{2\pi}\int_C \beta_o (S\alpha_{p_o} - k)\, ds \qquad (33)$$

For a linear machine, with the chromaticity compensated by sextupoles, this term amounts to zero. The second term in (28) is made of two parts: the first one comes from the variations of β induced by the sextupole distribution and contains also an intrinsic part which gives a curvature

of chromaticity even for a pure linear machine, not compensated by sextupoles. The second part is :

$$\bar{b} = \nu_o^2 \cdot \frac{1}{2\pi} \int_0^{2\pi} \beta_o^2 \left(S\alpha_{p_1} - S\alpha_{p_o} + K \right) d\phi \qquad (34)$$

Here again appears an intrinsic term adding to the curvature of chromaticity for a linear machine. When the linear chromaticity is compensated by sextupoles, the integral of K - S vanishes and we are left with :

$$\begin{aligned} \bar{b} &= \frac{\nu_o^2}{2\pi} \int_0^{2\pi} \beta_o^{5/2} \left(-\tilde{\alpha}_{p_o} + \nu_o^2 \sum_n \frac{F_n^1}{\nu^2 - n^2} \cdot e^{in\phi} \right) S \, d\phi \\ &= -2\nu_o^2 \cdot \Delta\xi + \nu_o^4 \sum_n \frac{(\beta^{5/2} \cdot S)_{-n} \cdot F_n^1}{\nu^2 - n^2} \end{aligned} \qquad (35)$$

Again F^1 contains an intrinsic part, and a part which depends on the sextupole distribution, this time through the induced variations of the α_p function.

3.2 Application to the SPS

The basic ingredient is the harmonic analysis of the following lattice functions: $\beta^2 \alpha_{p_o} S$, $\alpha_{p_o}^2 S$ and $\beta^{3/2} \alpha_{p_o} K$.

The interest of the analytic calculation is that it shows clearly how the sextupole distribution, through its Fourier harmonics, influences the non-linear ξ and hence how to eventually modify it to reduce the unwanted curvature.

So we will give in detail (Table I) the relative contributions of the most important harmonics n for the two main terms :

- the "βterm" $\quad 2 \cdot \frac{(\beta^2 \alpha_{p_o} S)_n}{n^2 - 4\nu^2}$
- the "$\alpha_p$term" $\quad -2 \cdot \frac{(\beta^{5/2} S)_n \cdot (\beta^{3/2} \cdot S/2 \cdot \alpha_{p_o}^2)_n}{\nu^2 - n^2}$

where (F)n means the nth Fourier component of the function $F(\phi)$.

One must be careful to carry out the summation to orders n much higher than those given here, as their total contribution is not at all negligible. Notice the following :

- "βterm" : the important harmonics are those close to $2.\nu = 53.2$. Hence the importance of harmonic 54, but also of harmonics 36 and 72, which are further away from the resonance condition, but still contribute a lot because of their greater (intrinsic) strength. The terms above and below resonance tend to cancel out, leaving a sum very close to the sole contribution

of harmonic 54. So one sees easily how to play with this term, either by reducing the strength of harmonic 54, or by changing the machine tune. It turns out that the main contribution comes from the following ("α_p") term, so this game is not very rewarding anyway.

- " α_p term" : here clearly trouble arises because the number of sextupoles (36) is too near to the ν value. Just doubling this number (72) should eliminate almost completely the contribution from this term (which is the most significant).

Table I

n	" β term"	" α_p term"
0		-.55
6	-.02	
12	-.03	
18	-.02	
24	-.03	
30	-.03	
36	-.68	1.34
42	-.06	
48	-.15	
54	.57	
60	.10	
66	.04	
72	.45	.17
78	.02	
84	.02	
90	.01	
96	.01	
102	.01	
108	.12	.07

Finally, let us give the results of the complete analytic calculations in the case of the "normal" machine (chromaticities = -1.3) and compare them to the results obtained from the AGS program (Table II).

Table II

$\Delta\nu_H/\delta^2$	analytic	AGS
Intrinsic (no sextupoles)	58	55
"β"	107	95
"α_p"	185	240
Total (compensated machine)	350	390

The agreement between analytic calculations and AGS runs is very good.

For the 10 GeV/c compensated machine, comparison between analytic calculations and AGS results or experimental data is complicated by the presence of sextupole errors in the magnets (see chapter 4). Nevertheless, results are in good agreement with experimental data (within the error bars).

In the vertical plane, the effect is much less pronounced. There are several reasons :

- the harmonic n = 54 of the LSD distribution is much smaller than in the horizontal case. Consequently, the "β" term is small and negative.

- the "α_p" term is also small because the influence of LSD sextupoles on α_p is small. In addition, interaction with the LSF sextupole effect gives a cross term of opposite sign which cancels out partially this effect.

Finally, analytic calculations give a vertical $\Delta\nu_v/\delta^2$ of 58, whereas the AGS program gives 85. Again the results are in reasonable agreement, if one considers that in this case many terms of opposite sign cancel out, and errors add up.

4. ANALYSIS OF THE SPS DATA

4.1 Fitting with AGS calculations

Both the horizontal and vertical chromaticities of the SPS before sextupole correction vary with time during the acceleration cycle: on top of the natural terms which come from the momentum dependance of the focusing strength of the machine quadrupoles, field proportional errors, remanent field and eddy currents in the vacuum chamber induce sextupolar fields which modify the machine chromaticity. This was taken into account in the computer simulation by putting in the AGS data sextupolar components S_{MBA} and S_{MBB} in the field of the main bending magnets MBA and MBB. These two parameters are adjusted such that the chromaticities calculated from the AGS output for $\Delta p/p = \pm 1‰$ are equal to the measured values. For instance, at 200 GeV and for the uncorrected chromaticities deduced from Fig. 5, one finds :

$$S_{MBA} = -.1298 \times 10^{-3}\ m^{-3} \quad - \quad S_{MBB} = -.0332 \times 10^{-3}\ m^{-3}$$

Here also these sextupole strengthes are normalized to the magnetic rigidity, according to (9). The effect of the chromaticity sextupoles can now be simulated by adding in the AGS data their normalized strength deduced from their measured currents. Comparison of AGS results with the 200 GeV measurements of Fig. 4 shows an excellent agreement as it can be seen on Fig. 8. Note that for the curve No. 2, the quadrupole gradients in the AGS data were slightly readjusted as compared to curve No. 1 in order to match the measured and calculated values of Q_H for the central orbit ($\Delta\bar{R} = 0$). On this figure, the error bars correspond to two standard deviations taken over ten measurements.

The same perfect agreement was also found for the other 200 GeV data of Fig. 5, in particular for a partially compensated horizontal chromaticity for which some curvature was experimentally observed.

One cannot perform exactly the same exercise at 10 GeV, where the uncorrected chromaticities are much more difficult to measure accurately: with no sextupole current, one looses most of the beam as soon as one tries to move it radially. One then had to apply some correction, measure the residual chromaticities and deduce from that the machine chromaticities, in order to estimate the stray sextupolar components S_{MBA}, S_{MBB} to be put in the bending magnets at this field level. In doing so one assumes that the effective partial correction given by the LSF and LSD sextupoles is equal to what can be calculated from their measured currents. This was verified by changing the sextupole settings and observing that the measured chromaticities were changing accordingly. As a result the uncorrected machine chromaticities at 10 GeV are :

$$\xi_H = -\ 2.130 \pm .05, \quad \xi_V = -.484 \pm .05$$

which can be obtained with the AGS program if one uses :

$$S_{MBA} = .5435 \times 10^{-3}\ m^{-3},\ S_{MBB} = .5573 \times 10^{-3}\ m^{-3}$$

Computer simulation was then performed as before and again a perfect agreement with all the available data at 10 GeV was obtained when the momentum deviation is not too large, i.e. $|\Delta p/p| \leq 8\ ^{0}/_{00}$. Fig. 9 shows two examples: the dashed curves No. 1 correspond to the nominal operation settings of the LSF and LSD at that time, whereas for the continuous curves No. 2, the sextupoles were firstly trimmed in order to flatten both Q-curves as much as possible near $\Delta \bar{R} = 0$. The dynamic aperture shown by curve No.4 of Fig. 2 was measured under the latter conditions. One should note that if the radial displacement exceeds $\pm$ 15 mm, part of the beam is lost and the measured Q-values have less meaning. One also has to take care of the separation between Q_H and Q_V to avoid any coupling during the beam displacement. Comparison with Fig. 8 shows that the curvature of Q_H is more pronounced at 10 GeV than at 200 GeV, as the relative strengthes of the sextupoles are higher because of the amount of correction needed.

Similar fittings were also done for several instants in the acceleration cycle, in particular near transition and at 80 GeV, and the same excellent agreement was always observed, as long as beam losses for large radial excursions do not perturb the measure of the Q's.

4.2 Chromaticity matrices

It follows from the previous chapters that if one neglects the non linear part of the chromaticity, i.e. its curvature, the effect of the LSF and LSD is equivalent to a change of chromaticity which to a first approximation is given by :

$$\begin{aligned} \Delta\xi_H &= -\frac{1}{4\pi}\left[\sum_{LSF}\beta_H\alpha_p\ell_{LSF}S_{LSF} + \sum_{LSD}\beta_H\alpha_p\ell_{LSD}S_{LSD}\right] \\ \Delta\xi_V &= -\frac{1}{4\pi}\left[\sum_{LSF}\beta_V\alpha_p\ell_{LSF}S_{LSF} + \sum_{LSD}\beta_V\alpha_p\ell_{LSD}S_{LSD}\right] \end{aligned} \qquad (36)$$

where the lattice functions β_H, β_V, α_p are taken for $\Delta p/p = 0$. These relations were used in the preceding paragraph to calculate the effect of the sextupole at 10 GeV. (36) can be inverted and written in a matrix form :

$$\begin{pmatrix} S^{*}_{LSF} \\ S^{*}_{LSD} \end{pmatrix} = B.\begin{pmatrix} S_1 & S_2 \\ S_3 & S_4 \end{pmatrix}.\begin{pmatrix} \Delta\xi_H \\ \Delta\xi_V \end{pmatrix} \qquad (37)$$

This is the relation presently used in operation for calculating the required sextupoles strengthes S^{*}_{LSF}, S^{*}_{LSD} in T/m^2 at a given bending field level B in order to obtain the corrections $\Delta\xi_H$, $\Delta\xi_V$ for the chromaticities. For the sake of simplicity, the same S_i coefficients, calculated from AGS output for the bare machine (i.e. with $S_{MBA} = S_{MBB} = 0$, and $S_{LSF} = S_{LSD} = 0$) are used

throughout the accelerating cycle. This assumption can be verified by calculating directly from the AGS output, the $\Delta\xi$ corresponding to $\Delta p/p = \pm 1\ ^{o}/oo$ and to different sextupoles strengthes. This was done for all the values of the stray sextupole components S_{MBA}, S_{MBB} obtained in the preceding paragraph and the results are given on Table III.

Although the operation parameters were determined for $Q_H = Q_V = 26.60$ while the other values are calculated for $Q_H = 26.620$ and $Q_V = 26.570$, the discrepancy does not exceed $1\ ^{o}/oo$ which is good enough for all practical purposes. One also sees that the S_i coefficients do not depend on the S_{MBA}, S_{MBB} but only on the working point Q_H, Q_V.

Table III

AGS simulation	$\xi_{H,N}$	$\xi_{V,N}$	$S_1 (m^{-2})$	$S_2 (m^{-2})$	$S_3 (m^{-2})$	$S_4 (m^{-2})$
bare machine	-1.2622	-1.2608	-36.1065	-7.7248	15.2324	70.5382
10 GeV	-2.1300	- .4836	-36.1131	-7.7572	15.2348	70.5517
21 GeV	+ .5428	-2.2168	-36.1218	-7.7964	15.2515	70.6285
83 GeV	- .5673	-1.7972	-36.1223	-7.7656	15.3137	70.6286
200 GeV	-1.0969	-1.3568	-36.1045	-7.7618	15.3061	70.6269
Operation val.			-36.0743	-7.7953	15.2452	70.5875

The chromaticities given in this table are those for the uncorrected machine. If one wants to have zero chromaticity, one must calculate S^{*}_{LSF}, S^{*}_{LSD} for $\Delta\xi_{H(V)} = -\xi_{H(V),N}$

One can similarly write a matrix relation which gives the stray sextupole components S_{MBA}, S_{MBB} as a function of the uncorrected machine chromaticities :

$$\begin{pmatrix} S_{MBA}(m^{-3}) \\ S_{MBB}(m^{-3}) \end{pmatrix} = 10^{-3} \cdot \begin{pmatrix} -1.1000 & -.5255 \\ +.6581 & 1.4499 \end{pmatrix} \begin{pmatrix} \Delta\xi_H \\ \Delta\xi_V \end{pmatrix} \qquad (38)$$

Here the $\Delta\xi_{H,V}$ are the difference between the uncorrected values $\xi_{H,N}$, $\xi_{V,N}$ and the corresponding natural terms calculated for the machine.

4.3 Chromaticity along the cycle

To complete this study we have to see if the linear part of the machine chromaticities vary during the acceleration cycle according to the simple model used so far, [5] :

$$\xi_{H,V}(t) = a + b.\frac{B_{inj}}{B(t)} + c.\frac{\dot{B}(t)}{B(t)} \qquad (39)$$

where B_{inj} is the injection field level and $\dot{B}(t)$ the time derivative of the bending field. The coefficients a and b can be calculated from the measured chromaticities on the 10 GeV and 200 GeV platforms and then c deduced from the other measurements near transition at 21 GeV and at 83 GeV (Table IV).

Table IV

	from measurements		for best fit	
	H	V	H	V
a	-1.043	-1.403	-1.042	-1.43
b	-1.087	+ .919	-1.020	+ .95
c (21 GeV)	+ .388	- .258	+ .38	- .33
c (83 GeV)	+ .438	- .334		

The determination of c, and hence the correction near the transition is not very precise : on top of the errors on the coefficients a and b, its accuracy is limited by the difficulty in measuring the chromaticities during the ramp. These coefficients were therefore used as a first approximation to correct the

chromaticities and the sextupoles were then trimmed all along the acceleration cycle in order to obtain a zero chromaticity at each instant. The best fit between (39) and the experimental curves $\xi(t)$ is obtained when one enters in the sextupole power supplies the coefficients given in the second part of Table IV. The differences with respect to the first set of coefficients come from some time lag in the tracking of (39) by the sextupole power supplies, but these values are in good agreement with previous measurements, [5].

The simple model (39) is therefore valid for the actual operation cycle and allows a chromaticity correction with an accuracy better than .1.

5. EXTRAPOLATION OF AGS SIMULATION

As the AGS program gives an excellent simulation of the non linear behaviour of the SPS chromaticity, one will use it to see how this effect can be compensated and what are its implications.

5.1 Correction of the curvature

It follows from chapter 3 that the first non linear term for the perturbated tune is quadratic in $\Delta p/p$ (eq. (28')), which is confirmed by the parabolic shape of the curves obtained by AGS. One can therefore try to correct the chromaticity curvature with octupoles, for instance the so-called Landau damping octupoles, LOD, which are located in front of the defocusing quadrupole No. 29 in each sextant. This is illustrated in Fig. 10, in which the continuous curves No. 1 represent the same AGS simulation at 10 GeV as in Fig. 9. One can find LOD settings which flatten the horizontal chromaticity (curves No. 2), but this is catastrophic for the vertical one, which is due to the bad LOD location. Moreover the required strength corresponds to about 60 A at 10 GeV which is prohibitive as it will introduce an enormous Q-spread, incompatible with the operating conditions.

It is more interesting to see the effect of the new octupoles which are to be installed in the near future: There will be one focusing LOFN upstream of the quadrupoles Nos. 8, 10, 22, 26 and 28 and one defocusing LODN before the quadrupoles Nos. 3, 5, 7, 25, 31, 33 and 35, in each sextant, [13]. These octupoles provide a much better correction as shown by the curves No. 3 of Fig. 10, thanks to their distribution. Nevertheless their normalized strengthes are not negligible - about 2 A per LOFN, with 30 octupoles in total - and it remains to be seen if this does not lead to undesirable effects.

By far the best correction is achieved when one increases the number of sextupoles: the curves No. 4 were obtained with one LSF in front of each focusing quadrupole and one LSD before each defocusing i.e. three times more sextupoles than now installed. This clearly demonstrate once more the effect of the sextupole distribution on the non linear chromaticity.

One may think of using the actual 36 sextupoles of each type but split in more than two families in order to minimize the main harmonics induced by their distribution. This was tried using the optimization program HARMON, [14] but the correction obtained was never better than with the future octupoles : for the SPS nominal working point, the betatron phase shift per magnetic period is close to 90° and because of the regular sextupole distribution, the main harmonics 36, 72 and 108 (see Table I) are always in phase, the only exception being the 54th harmonic. A working point near 20.6 would be much more favourable in this respect.

5.2 Applications to the p-$\bar{p}$ project

In its actual design stage, the proton-antiproton project [15] implies the injection of the antiprotons at 3.5 GeV into the SPS. At this field level, the remanent field effects become very important and it was experimentally found during the first 3.5 GeV injection tests, [16], that on top of other things the machine chromaticities were about :

$$\xi_H = -5.13 \ , \quad \xi_V = +2.15$$

which was determined from the amount of correction needed for the best transmission. Although these values are not very precise, they are good enough to simulate the SPS behaviour under these conditions, as shown on Fig. 11. When the above chromaticities are corrected, only with the actual sextupoles, curves No. 1, the chromaticity curvature is much more pronounced than at 10 GeV: the momentum excursion which corresponds to $\Delta Q_H = \pm .01$ is $\Delta p/p \simeq \pm 2.5$ °/oo as compared to $\pm$ 4.5 °/oo for 10 GeV. The Q_V curve also exhibits a strong curvature, whereas this was marginal at 10 GeV.

As before, the future octupoles can improve the situation. For the curves 2, their strengthes were ajdusted such that, [3] :

$$Q_{H,V}\left(\frac{\Delta p}{p} = -.001\right) + Q_{H,V}\left(\frac{\Delta p}{p} = +.001\right) = 2. * Q_{H,V}\left(\frac{\Delta p}{p} = 0\right)$$

which leads to a momentum acceptance of $\Delta p/p = \pm$ 3.5 °/oo for $\Delta Q_H = \pm .01$ This momentum acceptance is increased to $\pm$ 6.5 °/oo, curves 3, if one performs the octupole optimisation for $\Delta p/p$ = 5 °/oo, but note that this improvement is obtained with a relatively small change in the octupole strength as compared to curves 2, which means that this adjustment is critical. Also in both cases, the normalized LOFN strength is about four times greater than at 10 GeV which results in an enhancement of higher order terms.

Here again the best correction of the chromaticity curvature is achieved with one LSF and one LSD per magnetic period ; see the curves No. 4, for which the momentum acceptance is $\pm$ 10.5 °/oo. This correction has the further advantage of introducing no higher order terms.

One may also expect a somehwat stronger non linear chromaticity when a low beta section is inserted in LSS5 in order to increase the luminosity at the collision point. With the insertion parameters given in [15] AGS simulation shows indeed a change with respect to the regular machine (Fig. 12) but not as drastic as those obtained for larger storage rings, [11]. Even with a second insertion in LSS4, the tune variation with momentum is mainly parabolic and could be corrected with octupoles, but it remains to be seen if this type of correction has no detrimental effects on the stored beams, and is also feasible when switching on the insertions.

CONCLUSION

The non linear chromaticity which has been observed in the SPS mainly in the horizontal plane, has been completely explained with the existing perturbation theories. The perfect agreement between the experimental data and the simulation of the SPS with the AGS program allows to anticipate the consequences of this effect for the future SPS developments and to indicate ways for correcting it.

ACKNOWLEDGEMENTS

This study has benefitted from the constant support of B. de Raad and from discussions in the M.I.C. Meetings, in particular with E.J.N. Wilson. Some of the measurements reported here were performed during the normal SPS operation by P. Mills and W. Scandale.

REFERENCES

[1] SPS Commissioning Report No. 30, dated 15/11/76.
SPS Commissioning Report No. 63, dated 13/6/77.
SPS Improvement Report No. 104, dated 6/9/77.

[2] M. CORNACCHIA, Speculations on possible causes of beam loss in the SPS between injection and transition, SPS/ABT/MC/Int. 77-2, 7/6/77.

[3] E. KEIL, Y. MARTI, B.W. MONTAGUE, A. SUDBOE, AGS, the ISR computer program for synchrotron design, orbit analysis and insertion matching, CERN yellow report CERN 75-13.

[4] SPS Commissioning Report No. 28, dated 13/10/76.
SPS Commissioning Report No. 50, dated 16/2/77.

[5] M. CORNACCHIA and R. LAUCKNER, Measurement and compensation of chromaticity through SPS cycle. SPS Commissioning Report No. 65, dated 4/7/77. See also SPS Commissioning Report No. 14, dated 4/8/76.

[6] C. BOVET, R. GOUIRAN, I. GUMOWSKI, K.H. REICH, A selection of formula and data useful for the design of A.G. synchrotrons. CERN/MPS-SI/Int.D1/70-4.

[7] R. BOSSART, J. BOSSER, L. BURNOD, A. CHAPMAN-HATCHETT, E. D'AMICO, and P. MILLS, The SPS beam instrumentation and closed orbit correction. 1977 Particle Accelerator Conference, IEEE Trans. on Nuclear Science, vol NS-24, No. 3, p. 1733.

[8] R. LAUCKNER, The chromaticity sextupoles for the SPS main magnet system, CERN Lab II/MA-Int/75-6, 16/12/75.

[9] G. GENDREAU, A. LE DUFF, G. NEYRET, Spring study on accelerator theory, CERN, April 1972, AMC-1, p.35.

[10] P. MORTON, Derivation of non linear chromaticity by higher order "smooth approximation", Report PEP-221, Stanford, August 1976.

[11] H. WIEDEMANN, Chromaticity correction in large storage rings, Report PEP-220, Stanford, September 1976.

[12] E.D. COURANT, H.S. SNYDER, Theory of the alternating-gradient synchrotron, Ann. Phys. 3, 1-48, 1958.

[13] B. DE RAAD, private communication.
See also the SPS layout drawings 8002-010-1I and 8002-030-1H.

[14] M.H.R. DONALD, User's guide to harmon - RL-76-052, Rutherford Laboratory, May 1976.

[15] Design study of a proton-antiproton colliding beam facility, CERN/PS/AA 78-3, 21/10/78.

[16] V. RODEL, E.J.N. WILSON, Private communication.

[17] H. BRUCK, Accélérateurs circulaires de particules, Presses Universitaires de France, Paris 1966.

--oOo--

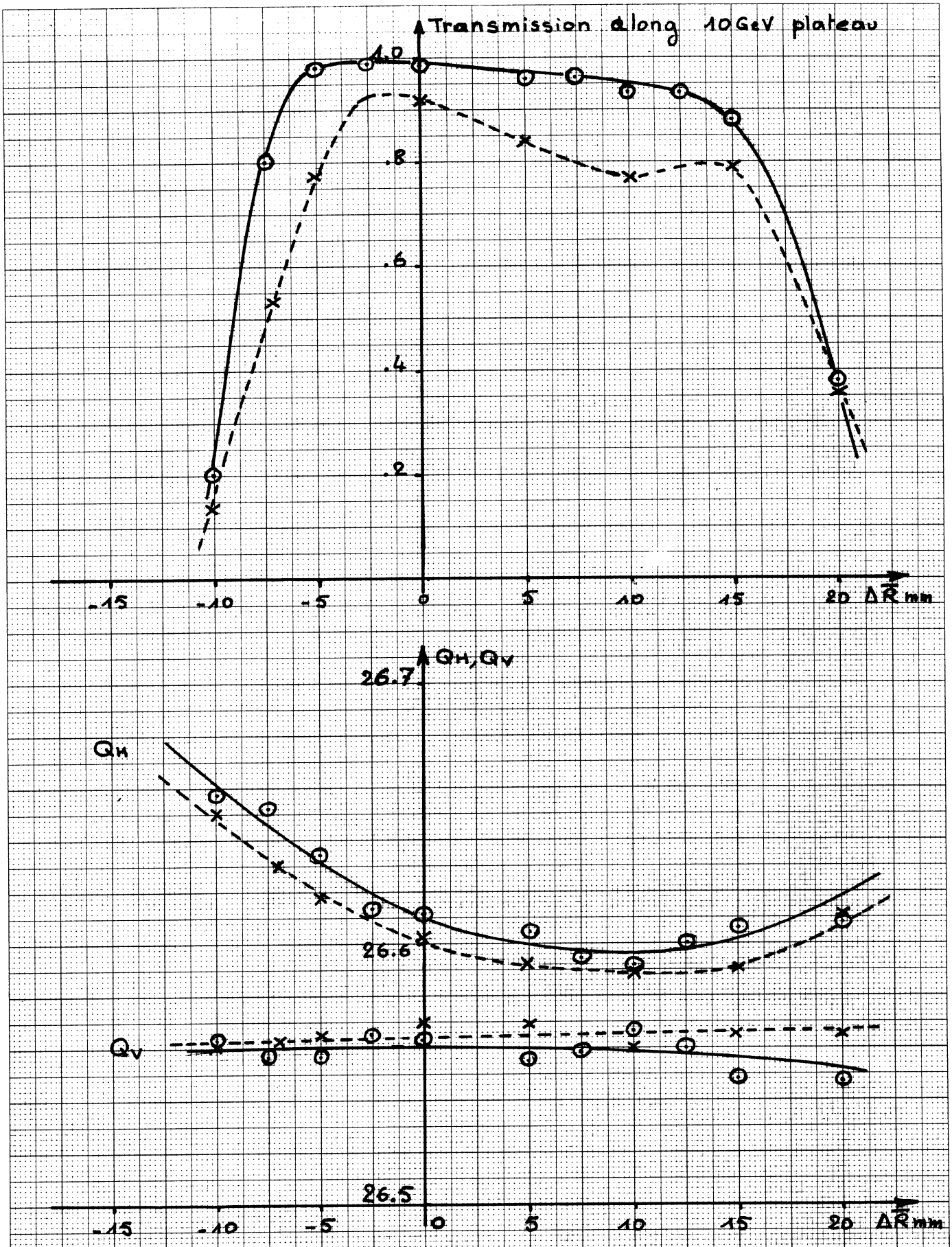

Fig 1: Variation of Q_H, Q_V & transmission vs mean radial position

--x-- $I_p = 4.10^{12}$ ppp - 10 GeV $\varepsilon_H = 1.2\pi$ $\varepsilon_V = .7\pi$ 17/11/77

—o— $I_p = 1.0 \times 10^{13}$ ppp - 10 GeV $\varepsilon_H = 2.2\pi$ $\varepsilon_V = .9\pi$ 29/11/77

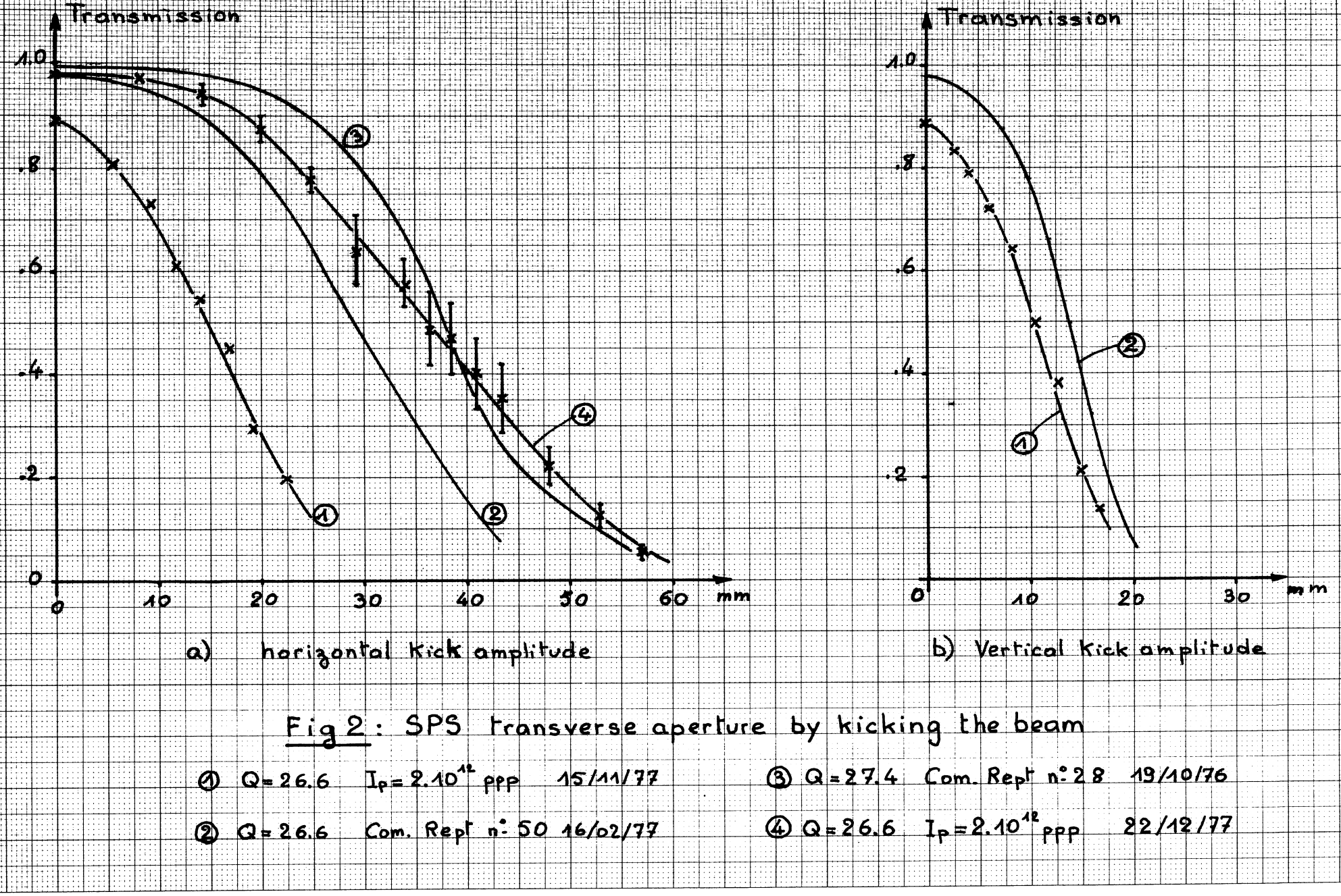

Fig 2: SPS transverse aperture by kicking the beam

① Q = 26.6 $I_p = 2.10^{12}$ ppp 15/11/77

② Q = 26.6 Com. Rept n°: 50 16/02/77

③ Q = 27.4 Com. Rept n°: 28 19/10/76

④ Q = 26.6 $I_p = 2.10^{12}$ ppp 22/12/77

SPS BP DISPLAY #20 T2=1200 10 MAR 78 15: 0:24

1 2 3 4 5 6

MOY= -13.399 SIG= 8.566 MIN -28.213 MAX 4.052

HOR

.960 MIN -8.913 MAX 3.578

VER

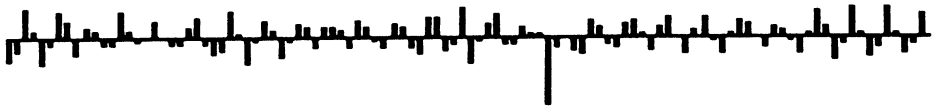

a) Displaced orbit at time of RF bump

SPS BP DISPLAY #32 T3=1400 T2=1200 10 MAR 78 15: 0:58

1 2 3 4 5 6

MOY= 11.461 SIG= 7.020 MIN -2.221 MAX 21.173

HOR

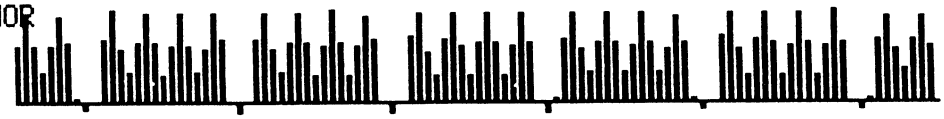

MOY= -.007 SIG= .260 MIN -1.128 MAX .431

VER

b) Differential orbit ($\Delta\bar{R}=0$ at $t=1400$)

Fig 3: Closed orbit for $\Delta\bar{R}=-10$mm (required)

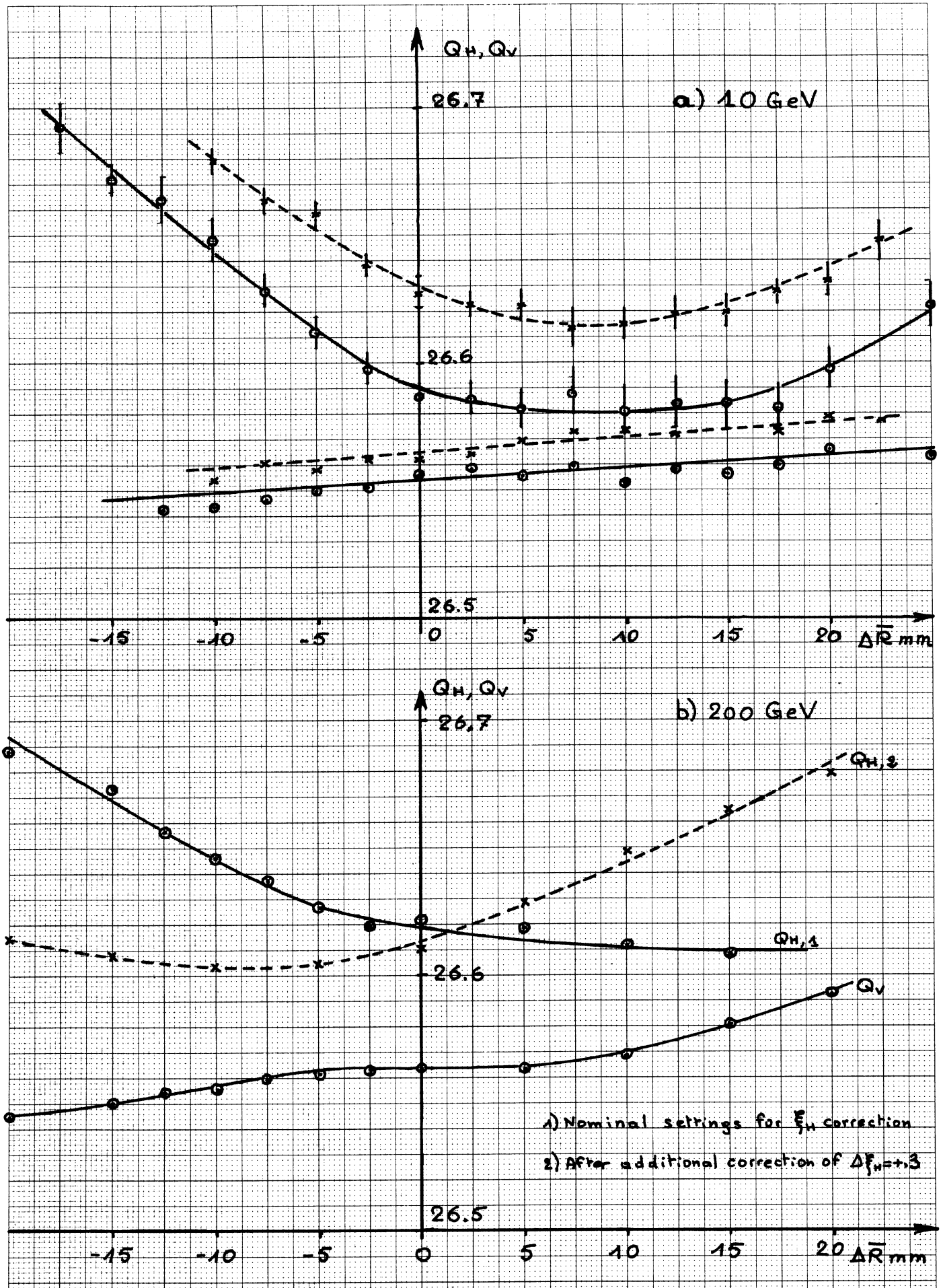

Fig 4: Curvature of SPS chromaticity

$I_p = 2.10^{12}$ ppp 5/12/77

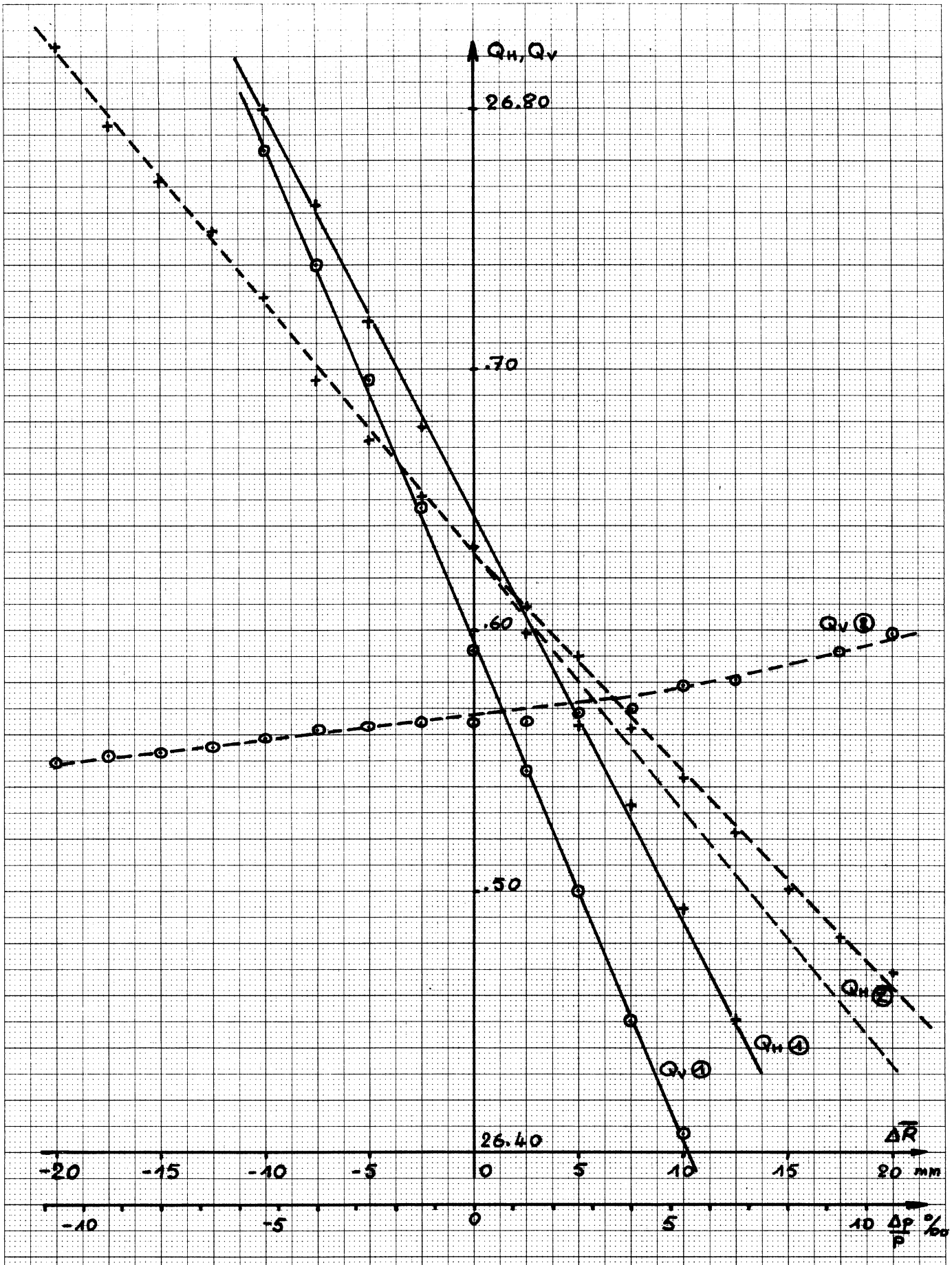

Fig. 5 : Chromaticity at 200 GeV (5/12/77)

① Bare machine, i.e. $I_{LSF} = I_{LSD} = 0$

② After a correction of $\Delta\xi_H = .5$ and $\Delta\xi_V = 1.464$

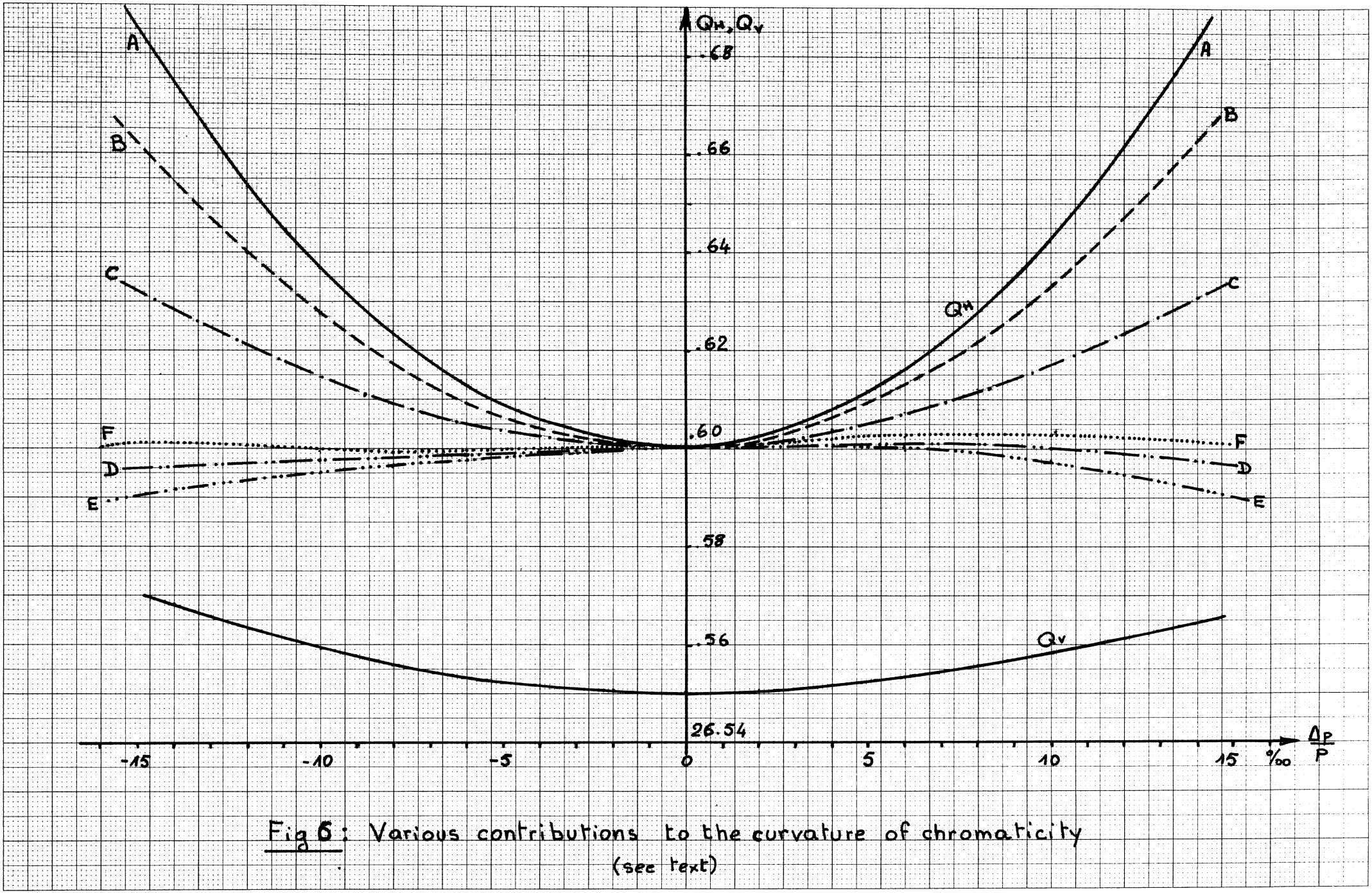

Fig 6: Various contributions to the curvature of chromaticity
(see text)

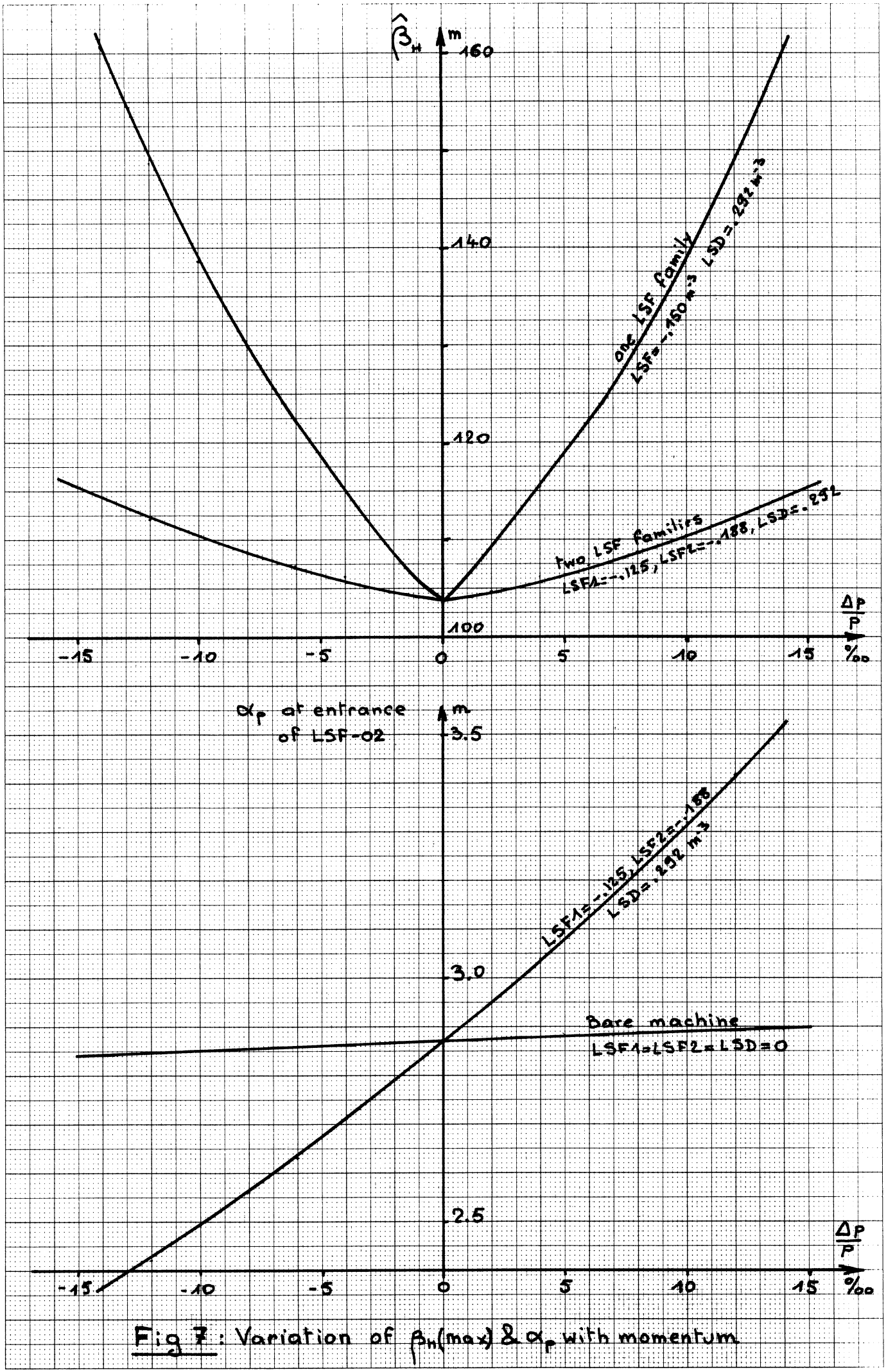

Fig 7 : Variation of β_H(max) & α_p with momentum

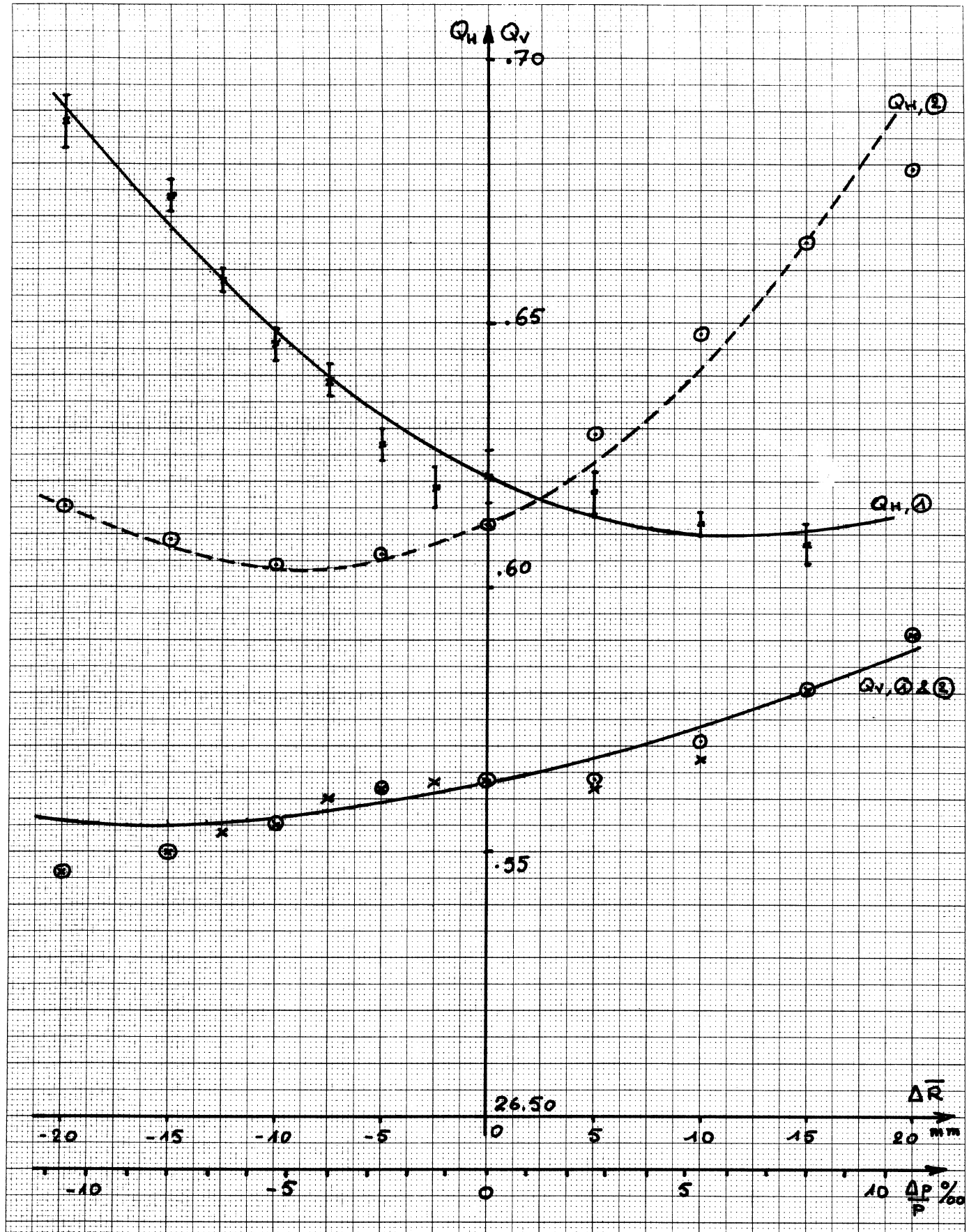

Fig 8 : Chromaticity at 200 GeV (5/12/77)

① × Meas with a correction of $\Delta\xi_H = .990$, $\Delta\xi_V = 1.466$

—— AGS simulation with LSF = $-.1237\ m^{-3}$, LSD = $.310\ m^{-3}$

② ⊙ Meas with a correction of $\Delta\xi_H = 1.290$, $\Delta\xi_V = 1.466$

– – – AGS simulation with LSF = $-.1494\ m^{-3}$, LSD = $.3203\ m^{-3}$

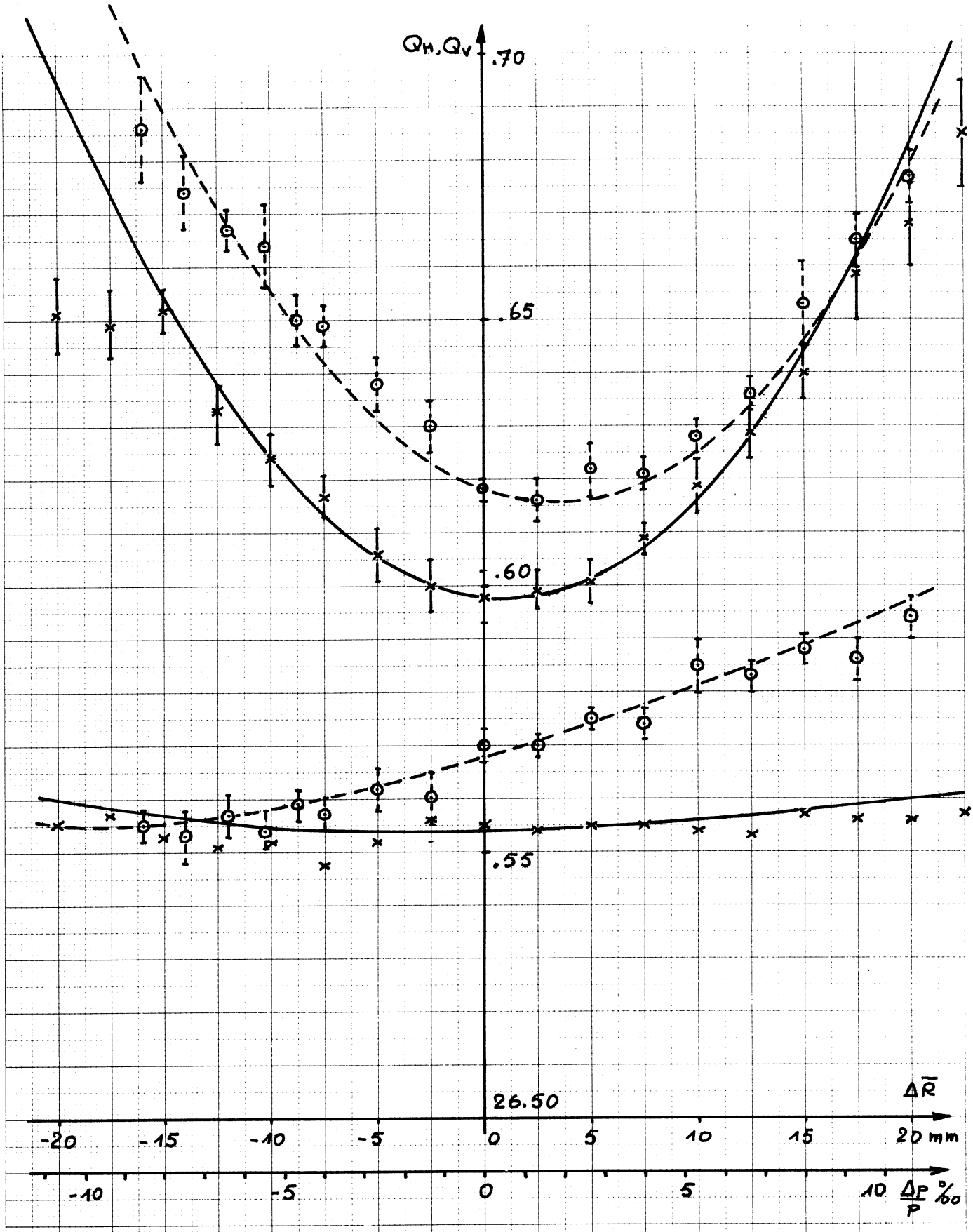

Fig. 9 : Chromaticity at 10 GeV (22/12/77)

① ⊙ Meas. with a correction of $\Delta\xi_{jH} = 2.147$, $\Delta\xi_{jV} = .563$

--- AGS simulation with LSF = $-.2091\ m^{-3}$ LSD = $.1910\ m^{-3}$

② × Meas. with a correction of $\Delta\xi_{jH} = 2.15$, $\Delta\xi_{jV} = .514$

—— AGS simulation with LSF = $-.2145\ m^{-3}$, LSD = $.1788\ m^{-3}$

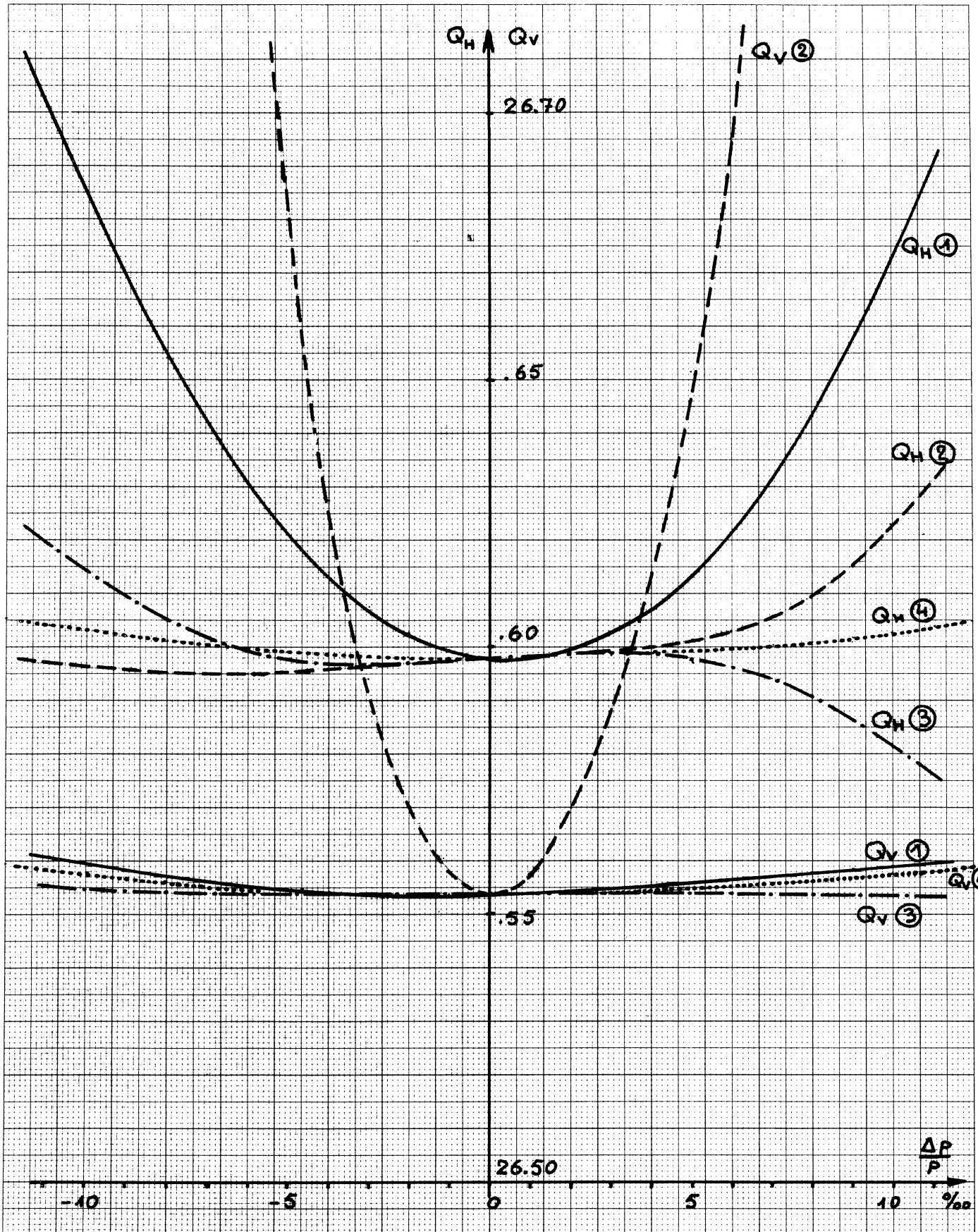

Fig.10 : Correction of chromaticity curvature at 10 GeV

① Actual curvature (No octupoles) LSF = -.2145 m^{-3}, LSD = .1788 m^{-3}

② Correction with actual Landau damping octupoles LOD = 217 m^{-4}

③ Correction with future octupoles : LOFN = 1.863 m^{-4}, LODN = -.641 m^{-4}

④ Correction with 1 LSF/LSD per QF/QD - No octupoles.

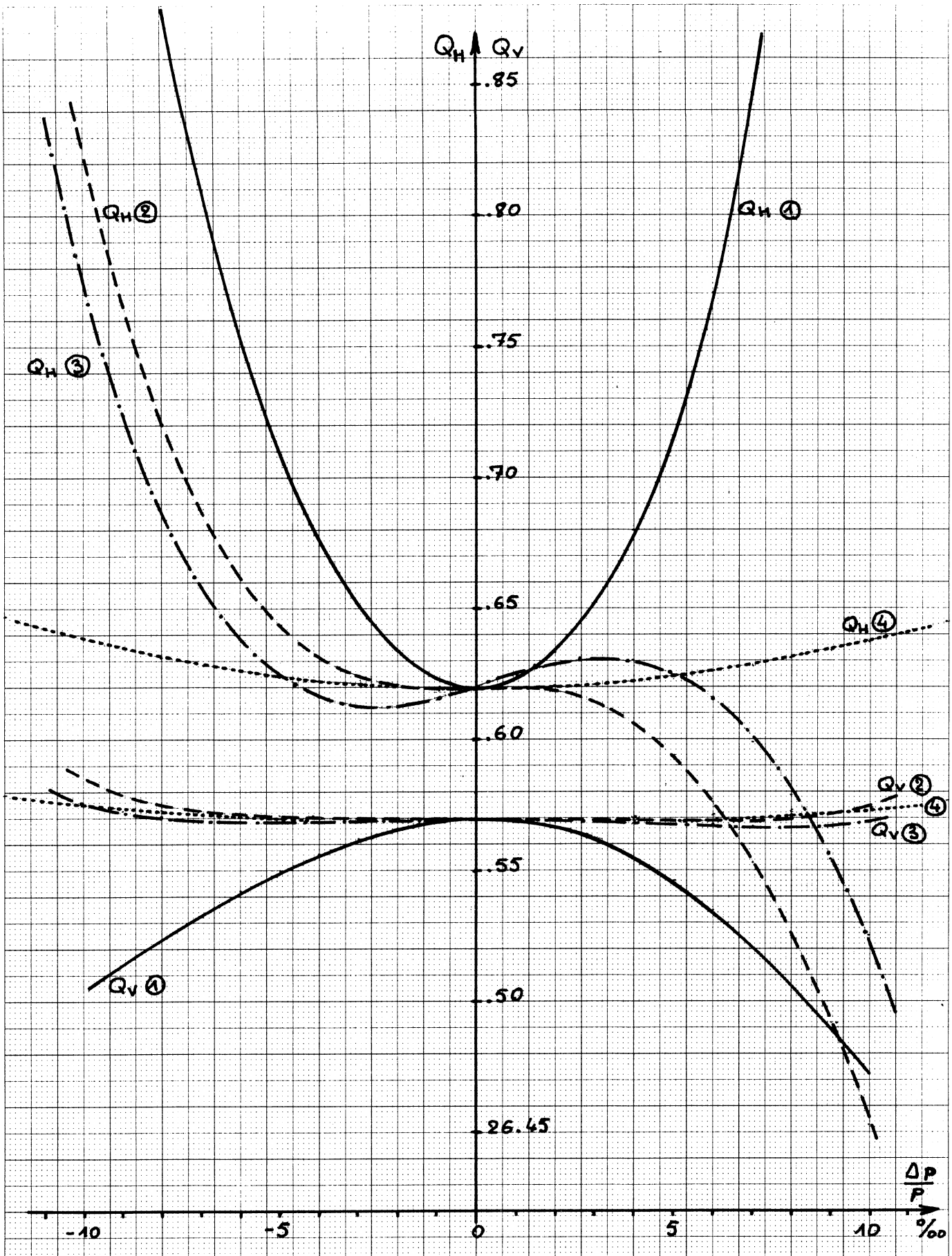

Fig. 11: Simulation of SPS chromaticity at 3.5 GeV

① ——— LOFN = LODN = 0, LSF = -.4539 m^{-3}, LSD = -.1977 m^{-3} (ξ_H = -5.13, ξ_V = 2.15)

② – – – LSF = -.4559 m^{-3}, LSD = -.1982 m^{-3}, LOFN = 7.742 m^{-4}, LODN = .0612 m^{-4}

③ —·— LSF = -.4735 m^{-3}, LSD = -.1983 m^{-3}, LOFN = 7.695 m^{-4}, LODN = .0346 m^{-4}

④ ····· One LSF/LSD per QF/QD - No octupoles

17 SEP. 1986

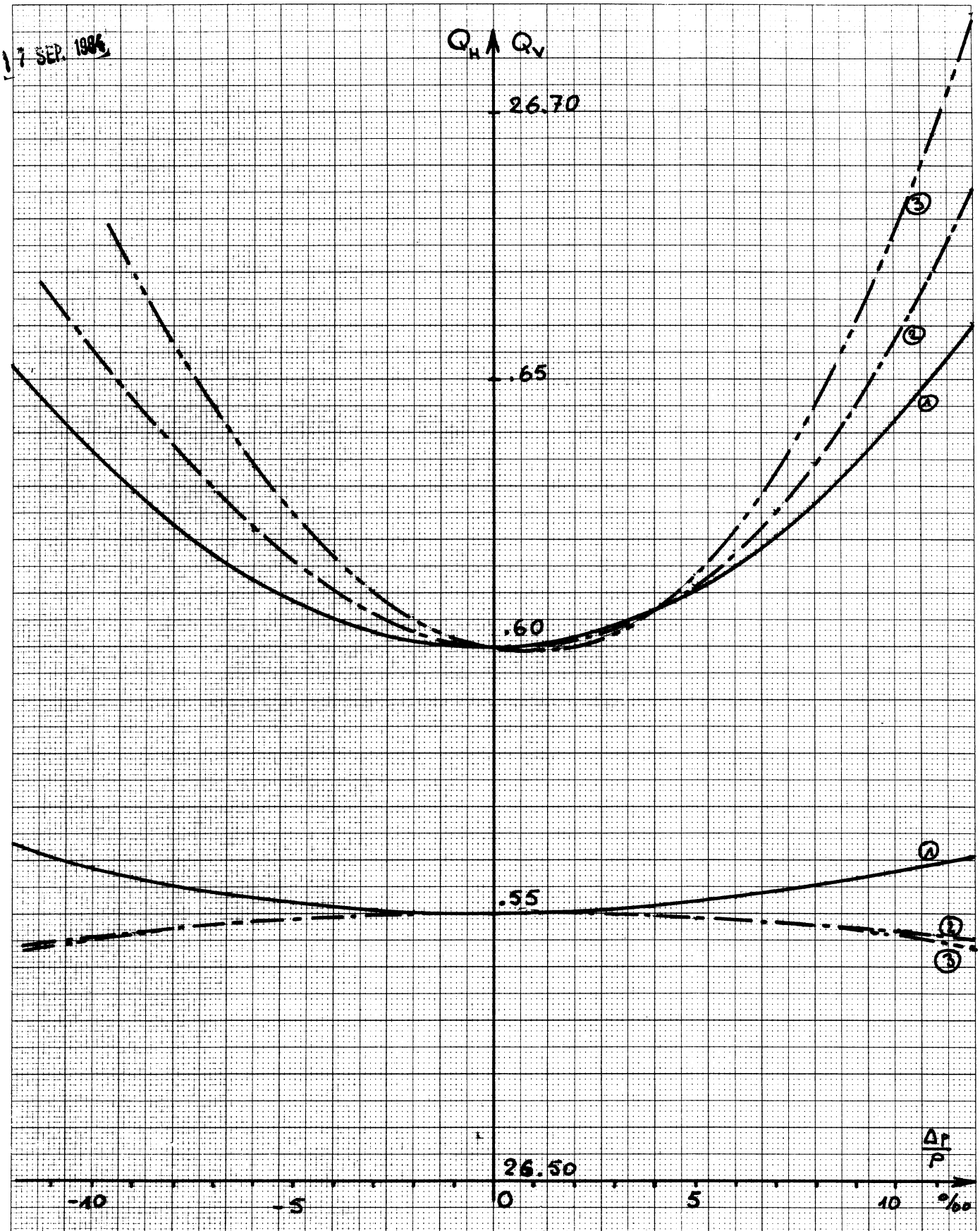

Fig 12: Simulation of SPS with low β insertions

① ——— Bare machine (no insertion). LSF = -.150 m^{-3}, LSD = .292 m^{-3}

② — — — One insertion in LSS5. LSF = -.167 m^{-3}, LSD = .321 m^{-3}

③ — · — · — Two insertions in LSS4&5. LSF = -.183 m^{-3}, LSD = .346 m^{-3}